MORPHOLOGY OF IMPURITIES IN STEEL AFTER DESULFURIZATION AND VACUUM DEGASSING

Tomasz Lipinski
University of Warmia and Mazury in Olsztyn, Poland
tomekl@uwm.edu.pl

Abstract. The properties of high-grade steel are influenced by a combination of factors, including the chemical composition, production technology and other factors. The quantity of impurities is also a key determinant of the steels properties. Inclusions may also play a negative important effect, which is dependent on their content, size, shape and distribution. An effective method for complete elimination of non-metallic inclusions has not been developed to date. There are, however, various techniques for reducing the quantity and the size of inclusions and controlling the quality of inclusions to minimize their adverse impact on the mechanical properties of high-grade steel. Steel was melted in a 100 ton converter and treated involved vacuum circulation degassing. The aim of this study was to determine the quantity and dimensional structure of inclusions in carbon steel melted in a converter subjected to desulfurization and vacuum circulation degassing. The results of the tests indicate that the quantity of submicroscopic non-metallic inclusions measuring up to 2 µm is the highest. Larger inclusions occupied greater volume in the alloy, but their number was lower. The dissipation coefficient is a sensitive parameter illustrating the strength of correlations between the oxygen content of steel and the volumetric share of oxide inclusions.

Keywords: steel, impurity, non-metalic inclusions, vacuum degassing, stereometry, morphology.

Introduction

Steel of various purity grades is manufactured for the production of elements that operate under different conditions. Steel used in structures, which are exposed to low loads, may contain significant amounts of impurities that do not compromise the functional parameters of steel [1-3]. The allowable impurity content of steel, the morphology of impurities and their influence on the steel strength (mainly under variable loads) have been analyzed by numerous authors [4-7]. Endogenous inclusions pose the greatest problem [8]. They include oxides, which are produced during reactions in the ingot mold, and sulfides, which are formed during the first stage of steel solidification [9; 10]. According to numerous research studies, endogenous inclusions of a similar number, size and distribution have a similar influence on the properties of steel [11]. The number of inclusions can be reduced by limiting the oxygen and sulfur content. In metallurgical processes, deoxidized steel can be supplied with oxygen diffused from slag or ladle lining [12-15]. Impurities from ladle lining are large in size and easy to remove mechanically. They can enrich steel in oxide impurities [16]. Steel can also be contaminated with exogenous impurities, such as erosion products from furnace or ladle lining. Non-metallic inclusions can be products of chemical reactions that occur in metals under exposure to fire retardant materials. They can also occur when steel comes into contact with ambient air [11; 15].

Despite years of research and analyses, our knowledge of the impact of non-metallic inclusions on the properties of steel elements is still ambiguous and limited. Most authors analyzed inclusions larger than 10 µm [3; 8; 17-19]. Methods for the production and out-of-furnace treatment of high-grade steel have been developed. The research results indicate that impurities are more effectively removed during out-of-furnace treatment than inside the furnace [20-25]. Studies investigating the morphology of submicroscopic impurities in structural steel characterized by high plasticity and high fatigue strength, such as the steel used in mining chains, are difficult to find.

Steel is highly effectively purified by vacuum degasification. In this process, vacuum acts on liquid steel in the ladle or on steel poured into ingot molds in a vacuum chamber. During vacuum degasification, the deoxidizing capacity of carbon increases above the surface of the metal with a decrease in pressure. In this process, oxides in non-metallic inclusions are reduced with the use of carbon dissolved in a molten steel bath. Inclusions are removed from the metal in reaction (1):

$$(MeO)_{const} + C = (CO)_{gas} + Me \,, \tag{1}$$
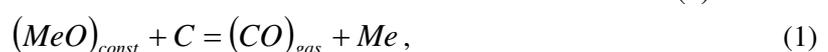
where $(MeO)_{solid}$ – solid metal oxide;
$(CO)_{gas}$ – gaseous carbon monoxide.

Large-sized inclusions are most effectively reduced. Steel degassed in a vacuum chamber is effectively purified of non-metallic inclusions [23]. Fine and evenly distributed non-metallic inclusions remain in the metal, whereas large impurities are nearly entirely eliminated. A reduction in the content of oxygen (through bonding with carbon) and sulfur (through evaporation) can be achieved by selecting optimal vacuum degassing processes. This problem was addressed in our study.

The aim of this study was to describe the distribution of non-metallic inclusions in structural steel melted in an oxygen converter and degassed in vacuum.

Materials and Methods

The study was carried out in an industrial setting with the aim of reproducing analytical results on an industrial scale. The analyzed material was constructional carbon steel. Steel was melted in a 100-ton oxygen converter and deoxidized by vacuum (RH treatment). Pig iron was ca. 25 % of the charge. Steel was cast continuously and square 100x100 mm billets were rolled with the use of conventional methods. Billet samples were collected to determine the chemical composition with the use of LECO analyzers, an AFL FICA 31000 quantometer and conventional analytical methods. Relative volume of non-metallic inclusions with the use of the extraction method and dimensions of impurities by inspecting metallographic specimens with the use of a Quantimet 720 video inspection microscope under 400x magnification were determined. Sample fragments corresponding to the area of 500 vision fields were analyzed. The relative volume of impurities was determined selectively by modifying the lower limit of the range determining the dimensions of the investigated inclusions to form two fractions.

The dimensions of non-metallic inclusions were equal to or higher than the adopted boundary values (minimum dimensions of the measured particle were equal 2 µm). The above approach enabled to determine the share of non-metallic particles at a level higher than and equal to the boundary value 2 µm. The applied measuring ranges were 5 and 10 µm respectively, too. Analytical calculations were performed on the assumption that the quotient of the number of particles on the surface divided by the area of that surface was equal to the quotient of the number of particles in volume divided by that volume [26].

The number of particles for the microscopically undetectable range was determined by chemical extraction where the content of all non-metallic particles was identified in the investigated steel. The particle content was the difference between the number of all inclusions and the number of inclusions measured at the lowest boundary value of 2 μm:

$$V_{d<2\,\mu m} = V_e - V_{\geq 2\,\mu m} \tag{2}$$

where $V_{d<2\,\mu m}$ – share of particles with a diameter smaller than 2 µm,
V_e – share of particles determined by chemical extraction,
$V_{\geq 2\,\mu m}$ – share of particles with a diameter larger than or equal to 2 µm.

The dimensions of non-metallic inclusions were described by stereometric parameters. The analysis focused on oxygen due to the predominance of oxygen inclusions. The dissipation of non-metallic inclusions in steel volume was described by the dissipation coefficient β (Eq. 3) that illustrates the correlations between the volume of oxide inclusions and the oxygen content.

$$\beta = O / V_i \tag{3}$$

where O – oxygen content of steel, vol. %,
V_i – relative volume of non-metallic inclusions evaluated in a metallographic analysis in the ith size interval or measuring range, vol. %.

The calculated number of inclusions in each size interval per surface area is presented by the coefficient of non-metallic inclusions (Eq. 4).

$$n_i = 4V_i / \pi d_{is}^2 \tag{4}$$

where d_{is} – average size of inclusion from the ith size interval, µm.

The percentage of sulfur-based inclusions was below the value of error in determinations of the percentage of oxygen-based inclusions; therefore, sulfur-based inclusions were excluded from further analyses. The main focus of the analysis was on oxygen-based inclusions.

Results and discussion

The chemical composition of heats is presented in Table 1.The content of sulfur and oxygen in steel from the examined heats is presented in Fig. 1. The impurity content of steel was low, the sulfur levels did not exceed 0.02 % (in melt number 5) and the oxygen levels did not exceed 0.003 % (in melt number 7). This confirms the effectiveness of the vacuum deoxidation process of steel.

Table 1

Chemical compositions of the research steel

Melt number	Chemical compositions, wt. %										
	C	Mn	Si	P	S	Cr	Ni	Mo	Cu	B	O
1	0.2	1.22	0.25	0.016	0.014	0.55	0.49	0.25	0.03	0.003	0.0023
2	0.23	1.18	0.22	0.018	0.017	0.5	0.51	0.22	0.02	0.003	0.0025
3	0.23	1.16	0.28	0.014	0.012	0.48	0.53	0.22	0.02	0.002	0.0028
4	0.24	1.13	0.27	0.018	0.018	0.56	0.5	0.26	0.02	0.003	0.0025
5	0.24	1.23	0.23	0.019	0.02	0.5	0.52	0.25	0.03	0.003	0.0025
6	0.25	1.21	0.23	0.02	0.016	0.56	0.52	0.24	0.02	0.002	0.0028
7	0.27	1.08	0.22	0.017	0.015	0.52	0.55	0.26	0.02	0.003	0.0030
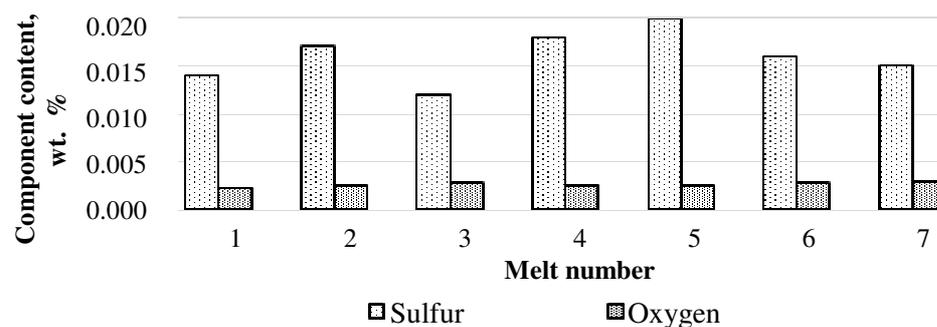
Fig.1. **Content of sulfur and oxygen on melt numbers of steel**

The total relative volume of non-metallic inclusions in the steel volume is presented in Fig. 2. Excluding heat 3, 6 and 7, the total relative volume of inclusions did not exceed 0.09% and in heat 3, 6, 7 did not exceed 0.12%.
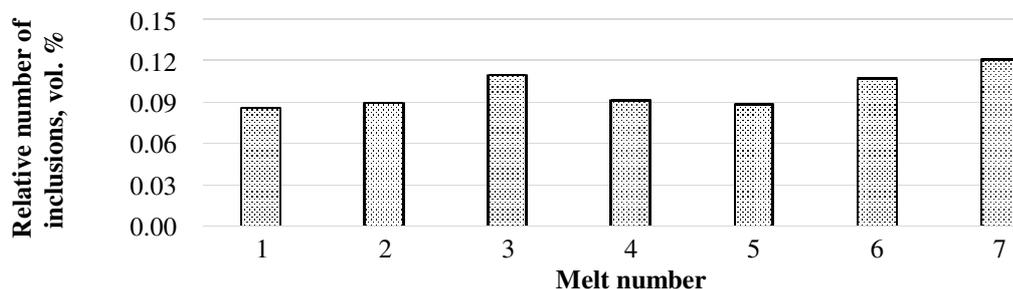
Fig. 2. **Relative volume of inclusions on melt numbers of steel**

The quantity of the non-metallic inclusions coefficient (Eq. 4) from 7 heats in different size intervals is presented in Fig. 3. The highest number of inclusions was reported in the fraction smaller than 2 µm, and was more than 15-, 60- and 80-fold higher than in successive intervals. The observed distribution of non-metallic inclusions reflects the efficiency of elimination processes by deoxidized by vacuum treatment in every size interval. Larger inclusions occupied greater volume in the alloy, but their number was lower. The increase in the size of impurities was generally accompanied by a decrease in their number.

The relative volume of non-metallic inclusions on melt numbers of steel in measuring range is presented in Fig. 4, and in size interval in Fig. 5. The percentage of non-metallic inclusions in the remaining measuring ranges indicates their volume for the size *w* and greater. For this reason, the volume ofinclusionsdecreases withtheirnarrowersize range. The volumetric share of small inclusions measuring up to 2 µm was smaller in threecases out ofseven than that of the remaining inclusions. The proposed approach to presenting the percentage of impurities in steel samples can be useful in analyses aiming to determine the effect of impurities of a given size or larger, for dimensionsgreater thanto the assumed size.
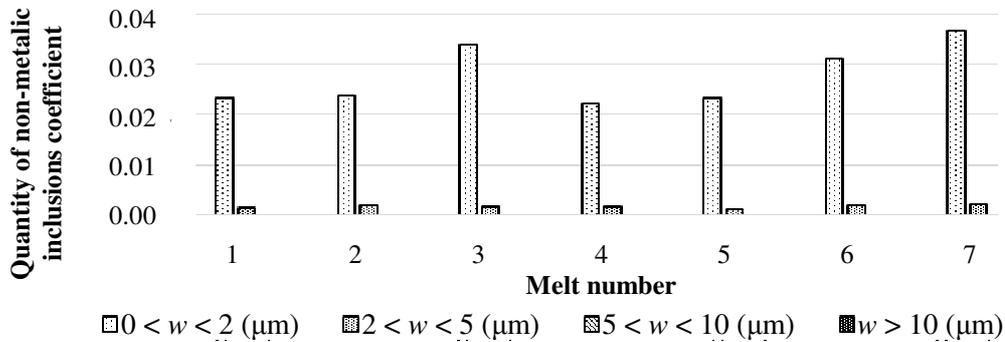
Fig. 3. **Quantity of non-metallic inclusions coefficient (n_i) in size intervals**
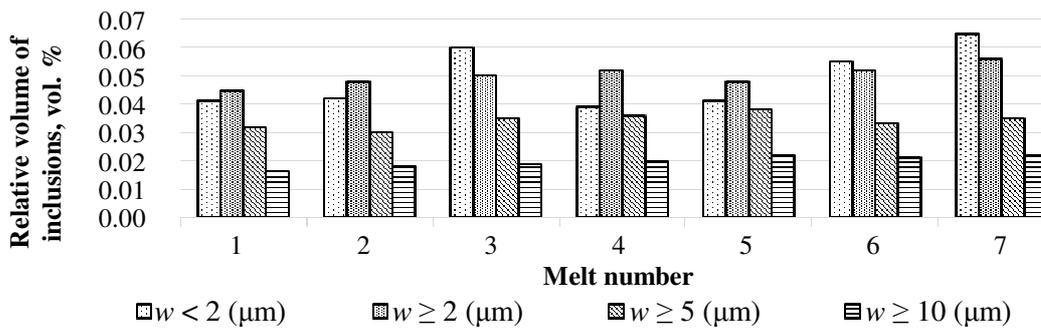
Fig. 4. **Relative volume of inclusions on melt numbers of steel in size interval**

The share of inclusions in every size interval was determined with the use of a histogram (Fig. 5).
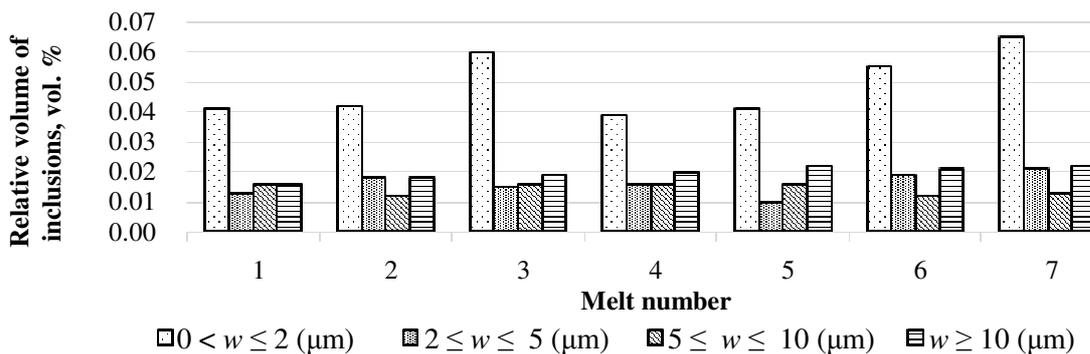
Fig. 5. **Size range relative volume of inclusions on melt numbers of steel in measuring intervals**

Fractionsequal to or largerthan 10 µm characterized by the highestvolumetric sharein 4meltsand thesizemeasuring up to 2 µm in3melts. When the above observation is compared with the results shown in Fig. 1, 2 and 3, it appears that the reported high share of submicroscopicinclusions in this size interval could be due to out-of furnace treatment of steel. A comparison of the values noted in this interval with the remaining intervals revealed small, but significantly statistical differences. The fraction with the highest volumetric share comprised inclusions of up to 2 µm, followed by inclusions measuring 2 to 5 µm.

The dissipation coefficient (Eq. 2) of non-metallic inclusions of steel in the measuring range is presented in Fig. 6. Analysis ofthe dissipation coefficientconfirms that the oxygen content of steel was correlated with the share of non-metallic inclusions. The dissipation coefficient was highest for small inclusions of up to 2 µm (for all 7 melts – Fig. 6).
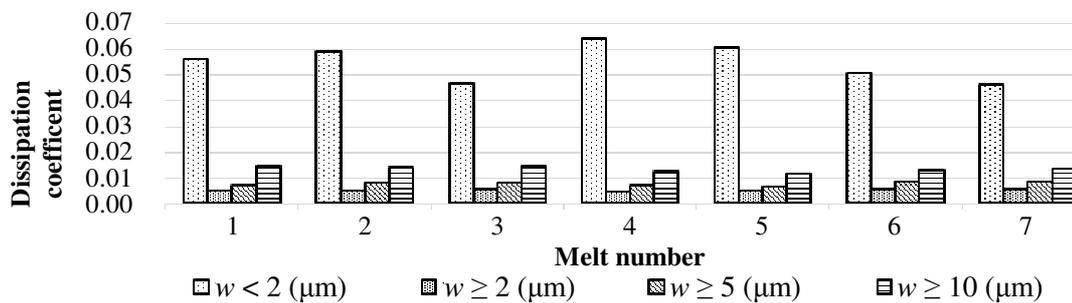
Fig. 6. **Dissipationcoefficient of non-metallic inclusions of steel in measuring range**

The dissipation coefficient increases when the oxygen content of different heats is constant and when the volume of impurities from different size classes decreases. The distance between inclusions from the same size class thus increases.

In this study, non-metallic inclusions measuring up to 2 µm had the highest volumetric and quantitative share of structural steel melted in an oxygen converter and deoxidized by vacuum. The above fractions were most numerous; therefore, they can be expected to influence the properties of the analyzed steel. Inclusions regarded as harmful in the literature (larger than 10 µm) are less frequently observed in the research steel, but their volumetric share can be significant on account of their large size. It should be noted, however, that the number of non-metallic inclusions in the steel degassed in vacuum is very small, which confirms theresults of the work [23]. Thus,the probability oftheir impact on properties is alsosmall. The dissipation coefficient is a sensitive parameter illustrating the strength of correlations between the oxygen content of steel and the volumetric share of oxide inclusions. The oxygen content of steel was correlated with the share of non-metallic inclusions.

The dissipationcoefficient is a sensitive indicator of the percentage of non-metallic inclusions in the microstructure of steel. The steel melted in a converter (Fig. 1) was characterized by a significantly lower oxygen content and a higher sulfur content than the steel melted in an arc furnace [24; 27].

Conclusions

1. The results of the tests indicate that the quantity of submicroscopic non-metallic inclusions measuring up to 2 µm is the highest.
2. Larger inclusions occupied greater volume in the alloy, but their number was lower.
3. The dissipation coefficient is a sensitive parameter illustrating the strength of correlations between the oxygen content of steel and the volumetric share of oxide inclusions.
4. The use of quantitative metallography in the analysis of non-metallic inclusions supports the determination of the size and inclusion structure, and enhances the methods of evaluating steel purity.

References

1. Evans M. H., Richardson A. D., Wang L., Wood R. J. K., Anderson W. B., Confirming subsurface initiation at non-metallic inclusions as one mechanism for white etching crack (WEC) formation, Tribology International, vol. 75, 2014, pp. 87-97
2. Hong Y., Lei Z., Sun Ch., Zhao A., Propensies of crack interior initiation and early growth for very-high-cycle fatigue of high strength steels, International Journal of Fatigue, vol. 58, 2014, pp. 144-151.
3. Ejaz N., Rizvi S.A., Cable failure resulted in the crash ofa trainer aircraft, Engineering Failure Analysis 17, 2010, pp. 394-402.
4. Mousavi S.M., Paavola J., Analysis of a cracked concrete containing an inclusion within homogeneously imperfect interface. Mechanics Research Communications,vol. 63,2015,pp. 1-5.

5. Lipiński T., Effect of the spacing between submicroscopic oxide impurities on the fatigue strength of structural steel. Archives of Metallurgy and Materials Vol. 60 Issue 3, 2015 (in print).

6. Ulewicz R., Quality control system in production of the castings from spheroid cast iron. Metalurgija Vol. 42 No. 1, 2003, pp. 61-63.

7. Spriestersbach D., Grad P., Kerscher E., Influence of different non-metallic inclusion types on the crack initiation in high-strength steels in the VHCF regime, International Journal of Fatigue, vol. 64, 2014, pp. 114-120

8. Moiseeva L. A., Moiseev B. P., Composition, Structure and Sources of Exogenous Inclusions in Steel, Steel in Translation , vol. 37, issue 7, 2007, pp. 607-613.

9. Wołczyński W., Constrained/unconstrained solidification within the massive cast steel/iron ingots. Archives of Foundry Engineering, vol. 10, 2010, pp. 195-202.

10. Ren Y., Zhang L., Yang W., Duan H., Formation and Thermodynamics of Mg-Al-Ti-O Complex Inclusions in Mg-Al-Ti-Deoxidized Steel. Metallurgical and Materials Transactions B 45, 2014, pp. 2057-2071.

11. Kiessling R., Non-metallic inclusions in steel, The Institute of Materials, London, UK 1978.

12. Wołczyński W., Concentration Micro-Field for Lamellar Eutectic Growth, Defect and Diffusion Forum 272, 2007, pp. 123-138.

13. Kowalski J., Pstruś J., Pawlak S., Kostrzewa M., Martynowski R., Wołczyński W., Influence of the Reforging Degree on the Annihilation of the Segregation Defects in he Massive Forging Ingots. Archives of Metallurgy and Materials, vol. 56, 2011, pp. 1029-1043.

14. Lipiński T., Wach A., The Effect of Fine Non-Metallic Inclusions on The Fatigue Strength of Structural Steel. Archives of Metallurgy and Materials Vol. 60, Issue 1, 2015, pp. 65-69,

15. Jiang M., Wang X., Pak J., Yuan P., In Situ Observation on Behaviors of CaO-MgO-Al2O3-SiO2 Complex Inclusions at Solid-Liquid Interface of Low-Oxygen Special Steel. Metallurgical and Materials Transactions B 45, 2014, pp. 1656-1665.

16. Seo W. G., Han W. H., Kim J. S., Pak J. J., Deoxidation equilibria among Mg, Al and O in liquid iron in the presence of MgO·Al2O3 spinel, ISIJ International, vol. 43, issue 2, 2003, pp. 201-208.

17. Yang G., Wang X., Huang F., Yang D., Wei P., Hao X., Influence of Calcium Addition on Inclusions in LCAK Steel with Ultralow Sulfur Content. Metallurgical and Materials Transactions B 46, 2015, pp. 145-154.

18. Luo S. J., Su Y. H., Lu M. J., Kuo J. C., EBSD analysis of magnesium addition on inclusion formation in SS400 structural steel, Material Characterization, vol. 82, 2013, pp. 103-112.

19. Barrie R. L., Gabbb T.P., Telesman J., Kantzos P.T., Prescenzi A., Biles T., Bonacuse P. J., Effectiveness of shot peening in suppressing fatigue crackingat non-metallic inclusions in Udimet® 720, Materials Science and Engineering A 474, 2008, pp. 71-81.

20. Lipiński T., Wach A., Dimensional Structure of Non-Metallic Inclusions in High-Grade Medium Carbon Steel Melted in an Electric Furnace and Subjected to Desulfurization. Solid State Phenomena 223,2015, pp. 46-53.

21. Lipiński T., Wach A., Size of Non-Metalic Inclusions in High-Grade Medium Carbon Steel. Archives of Foundry Engineering, vol. 14,issue 4, 2014, pp. 55-60.

22. Smirnov A. N., Efimova V. G., Kravchenko A. V., Flotation of Nonmetallic Inclusions during Argon Injection into the Tundish of a Continuous Casting Machine. Part 2, Steel in Translation, vol. 44, issue 1, 2014, pp. 11-16.

23. Gulyakov V. S., Vusikhis A. S.,Kudinov D. Z., Nonmetallic Oxide Inclusions and Oxygen in the Vacuum Jet Refining of Steel, Steel in Translation, vol. 42, issue 11, 2012, pp. 781-783.

24. Lipiński T., Wach A., Influence of Outside Furnace Treatment on Purity Medium Carbon Steel. 23rd International Conference on Metallurgy and Materials Metal 2014. Brno Conference proceedings 2014, pp. 738-743.

25. Lipiński T., Wach A., The influence of outfurnace processing on the exploatinal propriety the middle carbon high quality constructional steel, Archives of Fondry Engineering, vol. 10, issue 1, 2010, pp. 93-96.

26. Ryś J., Stereology of materials. FOTOBIT DESIGN, Krakow 1995 (in Polish).

27. Lipiński T., Wach A., Dimensional Structure of Non-Metallic Inclusions in High-Grade Medium Carbon Steel Melted in an Electric Furnace and Subjected to Desulfurization. Solid State Phenomena 223, 2015, pp. 46-53.